BUCKLING OF PILES WITH GENERAL POWER DISTRIBUTION OF LATERAL SUBGRADE REACTION

By M. A. Gabr,[1] Member, ASCE, J. J. Wang,[2] and M. Zhao[3]

ABSTRACT: A model for evaluating the critical buckling capacity of long slender friction piles is developed with lateral soil support included based on the concept of the subgrade reaction. A general power distribution of the coefficient of the subgrade reaction (k_h), with depth, is utilized in the model. The lateral force-deflection (P-y) behavior is assumed to be linear. A parametric study was conducted to demonstrate the effect of ω value, defining the distribution of the horizontal subgrade reaction, on the evaluated buckling capacity. In the case of the free top and fully embedded condition with embedment length (h) greater than 10 m, a 59% increase in the buckling capacity (P_{cr}) was predicted as ω was increased from 0 (constant horizontal subgrade reaction distribution) to 1 (linearly increasing horizontal subgrade reaction). Results also indicated that the boundary conditions at the pile tip have a minimal effect on P_{cr} when the nondimensional embedded length (h') exceeded 3.3 for the free top, 5.6 for the fixed-sway top, and 7.6 for the pinned-top condition. A comparison between a pile load test result reported in the literature and the model presented in this paper favorably verified the applicability of the developed model.

INTRODUCTION

The use of slender long piles extending a considerable distance above the ground line has increased over the past three decades. Examples of this type of foundation include piles supporting offshore structures and highway bridges in which the piles are extended to the structure's deck. In these cases, over half of the pile length can be unsupported. In general, long slender piles can fail in buckling mode under axial stresses below the yield point of the pile material, as presented by Golder and Skipp (1957) and Bergfelt (1957). Evidence of such behavior was also described by Brandtzaeg and Harboe (1957) for long piles that were extended above the ground surface. Experimental data from these studies showed that buckling failure of piles occurred suddenly with no obvious advance warning.

Several approaches were used for analyzing buckling of axially loaded piles. Early approaches by Brandtzaeg and Harboe (1957) and Golder and Skipp (1957) used Euler stability theory with the analysis verified using a limited number of buckling tests. Davisson and Robinson (1965) used the governing differential equation for buckling deflection to estimate critical loads with the assumption of constant and linearly increasing subgrade moduli. In this case, partially embedded piles were treated as free standing columns with fixed bases. Analysis using this approach was limited to a nondimensional embedded length (normalized pile length using soil-pile stiffness) of greater than 4. Reddy and Valsangkar (1970) used the energy method to develop a model for the estimation of critical buckling capacities of piles. Gabr and Wang (1994) developed a model for estimating the critical buckling loads of piles assuming uniform variation of the skin friction as a function of depth and nine cases of boundary conditions. In this study, the distribution of the modulus of horizontal subgrade reaction was restricted to the case of linearly increasing with depth.

In general, previous work on this subject was performed assuming the horizontal subgrade modulus to be either constant or linearly increasing with depth, as shown in Fig. 1. Applying a slight adaptation to Terzaghi's (1955) work, a common equation to describe the horizontal subgrade distribution can be expressed as follows [a constant $\zeta \equiv 1$ m is introduced to normalize the units, as suggested by Rowe (1956)]:

$$k_h = m_h z^{\omega} \zeta^{(1-\omega)} \tag{1}$$

where k_h = coefficient of horizontal subgrade reaction kN/m^3; m_h = ratio between coefficient of horizontal subgrade reaction and depth below ground surface (kN/m^4); ω = empirical power index equal to or greater than zero and describes distribution of k_h; and z = depth below ground surface.

Terzaghi (1955) recommended that the coefficient of subgrade reaction (k_h) can be assumed constant for cohesive soils and to increase linearly with depth for cohesionless soils. Davisson and Prakash (1963) suggested, however, that a power variation ($\omega = 0.15$) was a more realistic value for clays (presumably under undrained conditions), to allow for the plastic soil behavior near and at the surface. Reese and Matlock (1956) indicated that the adoption of piecewise linearly increasing distribution of subgrade modulus can account for soil yield and nonlinearity of piles in sand and soft clay. The Japanese Road Association (1976) recommended an ω value of 0.5 or within the range of 0.1–0.6 based on the results of their pile load tests. Kubo (1965) indicated that ω can be 0, 0.5, 1, or 2 depending on the soil and pile conditions.

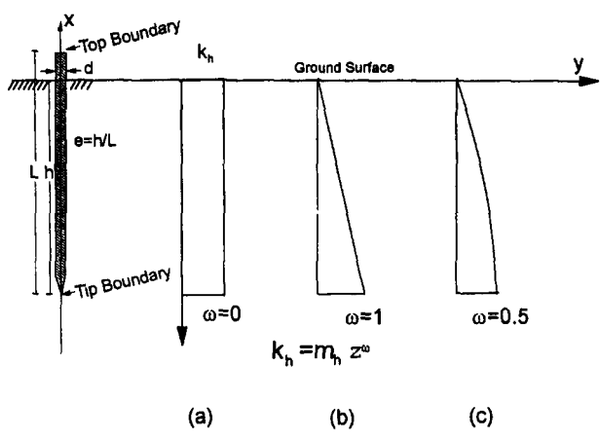

FIG. 1. Common Assumption of Subgrade Modulus: (a) Constant; (b) Linearly Increasing with Depth; (c) Nonlinearly Increasing with Depth

[1]Assoc. Prof., Dept. of Civ. and Envir. Engrg., West Virginia Univ., Morgantown, WV 26506.

[2]Engr., D'Appolonia Engrg. Div. of Ground Technol., Inc., 275 Center Rd., Monroeville, PA 15146.

[3]Assoc. Prof., Dept. of Civ. Engrg., Hunan Univ., Changsha, People's Republic of China.

Note. Discussion open until July 1, 1997. To extend the closing date one month, a written request must be filed with the ASCE Manager of Journals. The manuscript for this paper was submitted for review and possible publication on August 11, 1994. This paper is part of the ***Journal of Geotechnical and Geoenvironmental Engineering***, Vol. 123, No. 2, February, 1997. ©ASCE, ISSN 1090-0241/97/0002-0123–0130/$4.00 + $.50 per page. Paper No. 9037.

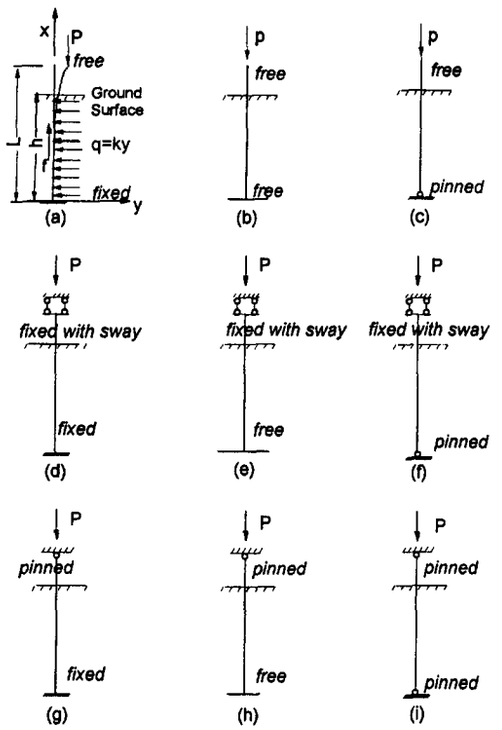

FIG. 2. Pile Deflection Models and Boundary Conditions

The several recommendations concerning the distribution of k_h can be commonly expressed by (1). However, no analytical model has been presented to estimate the critical buckling load (P_{cr}) of piles with a versatile subgrade reaction distribution that represents various soil conditions.

A buckling model is developed assuming a general power distribution of the coefficient of horizontal subgrade reaction with depth. The variation of the soil reaction with the lateral deflection from the buckling of the pile is presumed to be linear. This is based on assuming that buckling instability occurs at a relatively small lateral deformation of the pile material. The minimum potential energy concept is used to develop the model with suitable deflection functions selected using the Rayleigh-Ritz method. Nine combinations of pile top and tip boundary conditions are selected, as shown in Fig. 2 [after Gabr and Wang (1994)]. Fully embedded piles are treated as special cases of partially embedded piles. A parametric study is performed to investigate the buckling response of fully and partially embedded piles with various power distributions of the lateral subgrade reaction. Applicability of the developed model is demonstrated through the use of a case study reported in the literature.

LATERAL SUBGRADE REACTION

Analysis of the buckling behavior using the lateral subgrade reaction approach requires the knowledge of the variation of horizontal subgrade modulus and the soil reaction along the pile. The lateral pressure as a function of depth based on the subgrade reaction concept can be written as

$$p = m_h(h - x)^{\omega}\zeta^{1-\omega}y \tag{2}$$

where h = embedded pile length; x = distance from pile tip; and y = lateral deflection due to pile buckling. Referring to Fig. 2(a), the soil reaction as a function of depth is then expressed as

$$q(x) = pd = m_h d(h - x)^{\omega}\zeta^{1-\omega}y \tag{3}$$

where $q(x)$ = horizontal soil reaction per unit length of pile (kN/m); and d = pile width or diameter.

In this study, the variation of the soil reaction as a function of the lateral deflection is presumed to be linear, i.e., lateral pressure $p = ky$, where k is the lateral subgrade modulus at a given depth (note that k has units of force/length^2 and is computed by multiplying the coefficient of subgrade reaction k_h, force/length^3, by the pile diameter). This assumption is rationalized based on the fact that the model being developed is a stability rather than a laterally loaded pile model. In the pile buckling case, a relatively small material strain (on the order of 0.1%) can be interpreted as failure of the pile. Accordingly, the use of a linear soil reaction-lateral deflection relationship is justified.

PILE BUCKLING MODEL

The coordinates system for length and deflection is shown in Fig. 2(a). Deflection functions for the nine boundary conditions are chosen using the Rayleigh-Ritz method, as presented in Table 1. These deflection functions satisfy the various geometric boundary conditions of the analysis model.

The strain energy of the system due to the bending of the pile and elastic deformation of soil (U) and the potential energy of external loads (V) are expressed as

$$U + V = \frac{EI}{2}\int_2^L (y'')^2\,dx + \frac{1}{2}\int_0^h q(x)y\,dx - \frac{1}{2}\int_0^L P(x)(y')^2\,dx \tag{4}$$

where EI = flexural stiffness of pile; L = total pile length; h = embedded length of pile; $P(x)$ = axial force; n = number of half-wave of deflection function, integer; $y' = dy/dx$; and $y'' = d^2y/dx^2$.

Assuming a linearly increasing variation of the skin friction as a function of depth, the axial load in the pile is expressed as

$$P(x) = P\left[1 - \psi\frac{(h - x^2)}{h^2}\right] \quad (x \le h); \quad P(x) = P \quad (x > h) \tag{5a,b}$$

where P = axial load; and ψ = parameter defining influence of

TABLE 1. Deflection Functions and Boundary Conditions

Model number (1)	Boundary Conditions: Top (2)	Boundary Conditions: Tip (3)	Deflection functions (4)
a	Free	Fixed	$y = \sum_{n=1}^{\infty} c_n\left(1 - \cos\frac{2n-1}{2L}\Pi x\right)$
b	Free	Free	$y = c + \frac{x}{L}c_0 + \sum_{n=1}^{\infty} c_n \sin\frac{n\Pi}{L}x$
c	Free	Pinned	$y = \frac{c_0}{L}x + \sum_{n=1}^{\infty} c_n \sin\frac{n\Pi}{L}x$
d	Fixed-sway	Fixed	$y = \sum_{n=1}^{\infty} c_n\left(1 - \cos\frac{n\Pi}{L}x\right)$
e	Fixed-sway	Free	$y = c_0 + \sum_{n=1}^{\infty} c_n \sin\frac{2n-1}{2L}\Pi x$
f	Fixed-sway	Pinned	$y = \sum_{n=1}^{\infty} c_n \sin\frac{2n-1}{2L}\Pi x$
g	Pinned	Fixed	$y = \sum_{n=1}^{\infty} c_n\left(\cos\frac{2n+1}{2L}\Pi x - \cos\frac{2n-1}{2L}\Pi x\right)$
h	Pinned	Free	$y = c_0\left(1 - \frac{x}{L}\right) + \sum_{n=1}^{\infty} c_n \sin\frac{n\Pi}{L}x$
i	Pinned	Pinned	$y = \sum_{n=1}^{\infty} c_n \sin\frac{n\Pi}{L}x$

skin friction on pile axial force distribution with value between 0 and 1. A value of zero represents no skin friction.

Substituting (3) and (5) into (4), the following general equation is established:

$$U + V = \frac{EI}{2}\int_0^L (y'')^2\,dx + \frac{m_h d\zeta^{1-\omega}}{2}\int_0^h (h-x)^{\omega}y^2\,dx - \frac{P}{2}\int_0^L (y')^2\,dx + \frac{P\psi}{2h^2}\int_0^h (h-x)^2(y')^2\,dx \tag{6}$$

A conservative system is in equilibrium if the stored strain energy is equal to the work performed by the external loads, and can be expressed as follows:

$$\delta(U + V) = \frac{\partial(U + V)}{\partial C_i}\delta C_i = 0 \tag{7}$$

The symbol δ denotes change caused by virtual displacement; and C_i denotes constants of deflection function. δC_i = arbitrary variational displacement. Applying the minimum potential energy principle and since δC_i is arbitrary

$$\frac{\partial(U + V)}{\partial C_i} = 0 \tag{8}$$

Substituting (6) into (8), the following equation is obtained:

$$\int_0^L y''\frac{\partial y''}{\partial C_i}\,dx + \alpha^5\zeta^{1-\omega}\int_0^h (h-x)^{\omega}y\frac{\partial y}{\partial C_i}\,dx - \frac{P}{EI}\int_0^L y'\frac{\partial y'}{\partial C_i}\,dx + \frac{P\psi}{EIh^2}\int_0^h (h-x)^2y'\frac{\partial y'}{\partial C_i}\,dx = 0 \tag{9}$$

where $i = 0, 1, 2, \ldots, n$; n = half-wave number of deflection function; and α = coefficient of pile-soil compliance, or relative stiffness, and is defined as

$$\alpha = \sqrt[5]{\frac{m_h d}{EI}} \tag{10}$$

Substituting the deflection functions shown in Table 1 into (9) and performing the integration, a set of homogeneous linear equations in terms of C can be obtained. This system possesses nonzero solutions only if the determinant of the coefficient matrix is equal to zero. Appendix I presents determinants of the coefficient matrices [(14), (20), and (25), respectively] and defines the components for the cases of free-fixed, fixed with sway-free, and pinned-fixed.

The determinants expressed in (14), (20), and (25) are symmetric along the diagonal with P' [nondimensional parameter defined by (15)] being unknown. Expanding the determinant for each case, an algebraic equation of the nth, or $(n + 1)$ degree in terms of P' can be obtained. This equation is referred to as the characteristic equation of the system. The nth or $n + 1$ root of this equation is the eigenvalues.

The Jacobi Rotation method is used to find the eigenvalues for the coefficient determinants. The smallest root of the solution provides P' for this model. The other roots correspond to higher buckling modes. Once P' is obtained, the critical buckling capacity is defined as

$$P_{cr} = \frac{\Pi^2 EI}{L^2}P' \tag{11}$$

or in terms of equivalent buckling length, L_e

$$P_{cr} = \frac{\Pi^2 EI}{L_e^2} \tag{12}$$

where

$$L_e = \frac{L}{\sqrt{P'}} \tag{13}$$

Solutions of the determinant equations are implemented in the computer program GABPC (General Axial Buckling Pile Capacity). Using this program, the solution for the equivalent length, L_e, is obtained for the various boundary conditions utilized for the model development.

PARAMETRIC STUDY

A parametric study is conducted to investigate the effect of key analysis parameters on the buckling capacity of piles and to demonstrate a simplified methodology for estimating the critical buckling loads. For the sake of this study, the following nondimensional parameters are used: $e = h/L$, defines an embedment ratio; $L' = \alpha L$, nondimensional total length of pile; $h' = \alpha h$, nondimensional embedded length; and $L_e' = \alpha L_e$, nondimensional equivalent buckling length.

The value of e is varied from 0.5 to 1 with the value of 1 representing a fully embedded pile. For each boundary condition combination, three different ω values of 0, 0.5, and 1 are utilized. For $\omega = 0$, $m_h = 53$ MN/m^4 (representing the stiff clay condition) is used; for $\omega = 0.5$, $m_h = 34$ MN/m^4 (representing the dense sand condition) is used; and for $\omega = 1$, $m_h = 20$ MN/m^4 (representing the medium sand condition) is used. These m_h values conform to the values presented by Terzaghi (1955). Other key soil and pile parameters assumed in this analysis are $EI = 1.4 \times 10^6$ kN/m^2 (assuming concrete pile concrete), diameter = 0.75 m, and $\Psi = 0.5$ (median friction value).

Figs. 3–5 show the variation of the nondimensional equivalent buckling length L_e' as a function of h' for the nine boundary conditions considered in this model and use ω values of 0 and 0.5 (please note that these figures are drawn using different scales). Cases shown in these figures can be compared

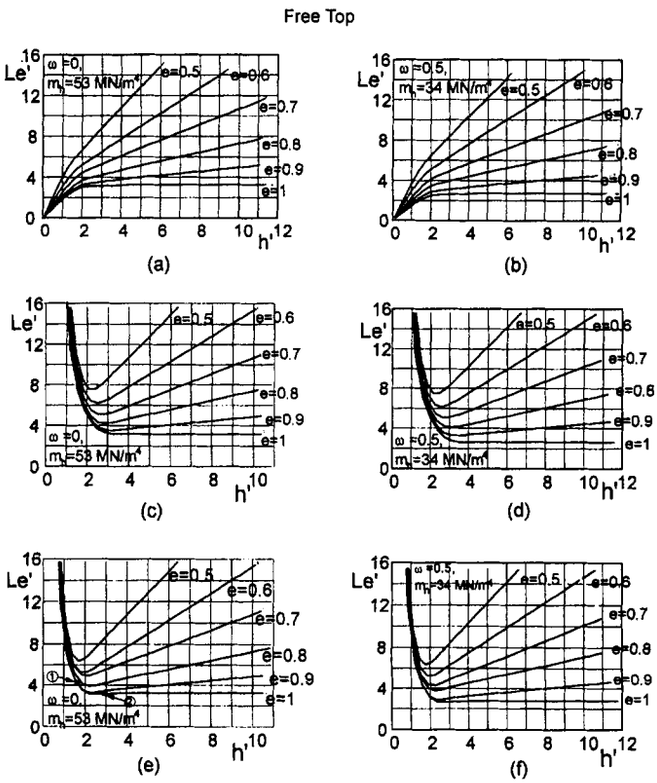

FIG. 3. Nondimensional Equivalent Buckling Length (L_e') versus Nondimensional Embedded Length of Pile (h') As Function of e (h/L) with Free Top and: (a) Fixed Tip, $\omega = 0$; (b) Fixed Tip, $\omega = 0.5$; (c) Free Tip, $\omega = 0$; (d) Free Tip, $\omega = 0.5$; (e) Pinned Tip, $\omega = 0$; (f) Pinned Tip, $\omega = 0.5$

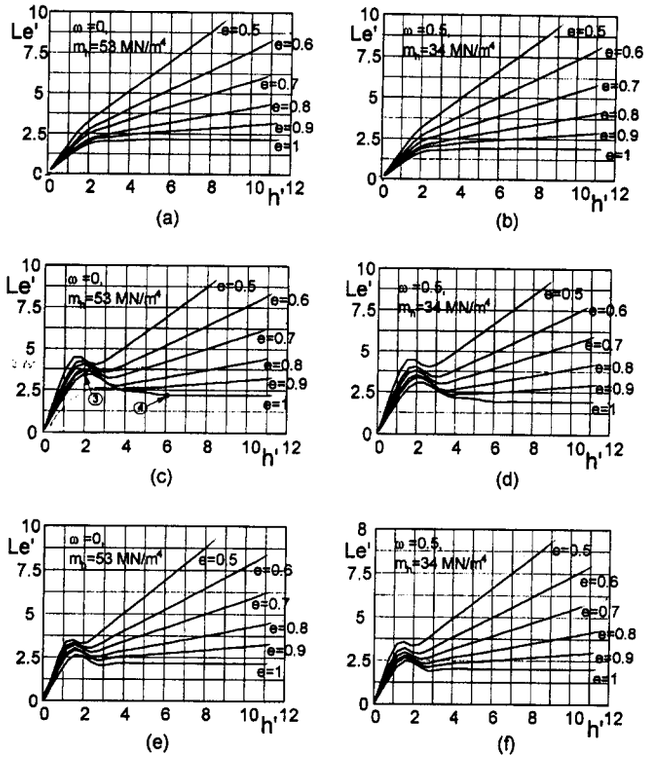

FIG. 4. Nondimensional Equivalent Buckling Length (L'_e) versus Nondimensional Embedded Length of Pile (h') As Function of e (h/L) with Fixed-Sway Top and: (a) Fixed Tip, $\omega = 0$; (b) Fixed Tip, $\omega = 0.5$; (c) Free Tip, $\omega = 0$; (d) Free Tip, $\omega = 0.5$; (e) Pinned Tip, $\omega = 0$; (f) Pinned Tip, $\omega = 0.5$

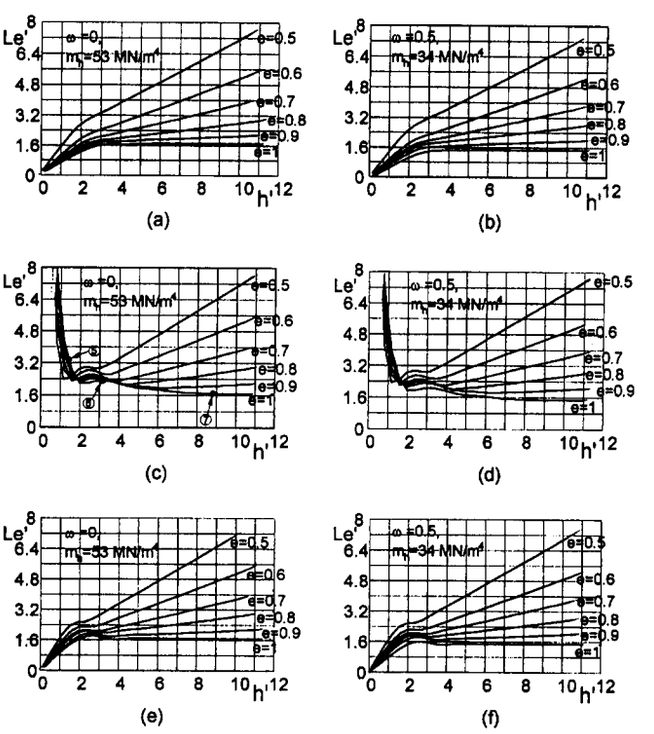

FIG. 5. Nondimensional Equivalent Buckling Length (L'_e) versus Nondimensional Embedded Length of Pile (h') As Function of e (h/L) with Pinned Top and: (a) Fixed Tip, $\omega = 0$; (b) Fixed Tip, $\omega = 0.5$; (c) Free Tip, $\omega = 0$; (d) Free Tip, $\omega = 0.5$; (e) Pinned Tip, $\omega = 0$; (f) Pinned Tip, $\omega = 0.5$

with cases presented by Gabr and Wang (1994) in which the subgrade reaction distribution was assumed linearly increasing with depth ($\omega = 1$).

As shown in Figs. 3(a,b), 4(a,b), and 5(a,b), which represent the cases of the fixed-tip boundary condition and free top, fixed-sway, and pinned-top boundaries, respectively, the L'_e increased as a function of increasing h'. This increase in L'_e indicated a decrease in P_{cr} with increasing the length of the pile. In the case of full embedment, this decrease in P_{cr} was less than 1% as h' exceeded the value of 3. However, as the embedment ratio (e) of the pile was decreased from 1 to 0.5, higher L'_e and, therefore, lower P_{cr} values were calculated for piles with $e < 1$.

In the case of boundaries representing free-free [Fig. 3(c,d)] and free-pinned [Fig. 3(e,f)] conditions, the value of L'_e tended to be infinite as h' approached a value less than 1. Infinite L'_e implies a $P_{cr} = 0$. The value of L'_e decreased as h' was increased up to a critical h' value [a first buckling mode corresponding to this behavior is presented in Fig. 6(a)]; after which L'_e increased as a function of h' [a first buckling mode corresponding to this behavior is presented in Fig. 6(b)]. The decrease in L'_e as h' is increased can be attributed to the difference in the buckling modes. For the case presented in Fig. 6(a), the presence of inflection points reduces the critical buckling length. Consequently, the contribution of the lateral soil stiffness to the buckling stability is less for the mode with the inflection points as compared to the case presented in Fig. 6(b). This leads to a higher L'_e and therefore a lower P_{cr}. The decrease in L'_e was estimated to be a function of the embedment ratio. For $e = 0.5$, the critical h' value was estimated to be 2, and for $e = 1$ the critical h' value was estimated to be 3. Similar behavior was computed for the pinned-free case [Fig. 5(c,d)].

In the case of fixed-sway top (where the pile is free to dis-

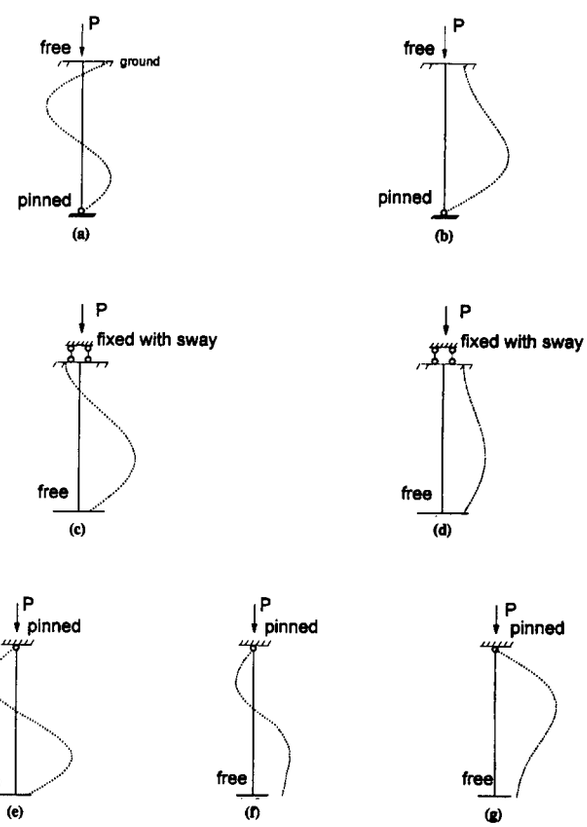

FIG. 6. First Pile Buckling Modes ($e = 1$) Corresponding to: (a) Point 1 in Fig. 3(e); (b) Point 2 in Fig. 3(e); (c) Point 3 in Fig. 4(c); (d) Point 4 in Fig. 4(c); (e) Point 5 in Fig. 5(c); (f) Point 6 in Fig. 5(c); (g) Point 7 in Fig. 5(c)

place laterally with the tangent to the elastic curve remaining vertical), free-tip [Fig. 4(c,d)], and pinned-tip [Fig. 4(e,f)] conditions, the general trend of increasing L_e' with h' was interrupted by a region of decreasing L_e' for h' values between 1 and 3. This resulted in the "hump" shape shown in these figures. The first buckling mode corresponding to the "hump" point [labeled "3" in Fig. 4(c)] for the case of free tip and $e = 1$ is shown in Fig. 6(c). For the sake of comparison, the first buckling mode for a general point on the same curve [labeled "4" in Fig. 4(c)] is shown in Fig. 6(d). The difference in the buckling modes may explain the "hump" shape of this curve. In this case, the first buckling mode at the hump point contained an inflection point, as shown in Fig. 6(c). While the presence of an inflection point reduces the critical buckling length, it also means less contribution from the lateral soil stiffness to the buckling stability. In comparison, the buckling mode for the general point [labeled "4" in Fig. 4(c)] is such that the contribution of the soil lateral stiffness is along the whole length of the pile, which leads to a lower L_e and, therefore, a higher P_{cr}.

Fig. 5(a–f) represents cases with the pinned top condition. The first buckling modes for three cases located in different regions of the L_e'-h' curve in Fig. 5(c) are presented in Fig. 6(e–g).

As previously explained, the significantly different modes account for the different trends existing in the curve, as the soil stiffness contribution to the buckling stability is dependent on the critical buckling length.

Similar to previous predictions by Gabr and Wang (1994), the effect of the skin friction on the equivalent buckling capacity is found to be insignificant for the various distributions of the subgrade reaction. Within a Ψ range of 0–1, less than 10% variation in the buckling capacity was predicted.

The number of terms (n values in the deflection functions) used for all calculations in this paper is 50. However, less than a 1% difference in L_e' values was found by using $n = 26$ as compared to $n = 50$. Therefore, 26 can be considered as the number of terms to obtain accurate buckling capacities.

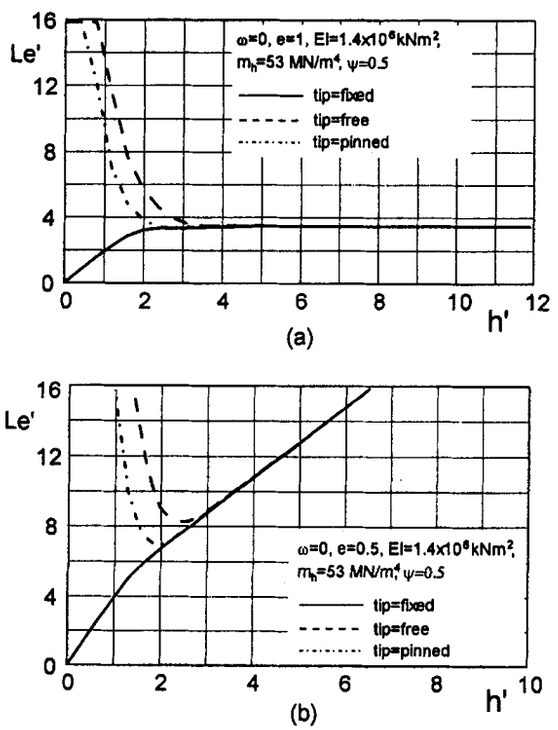

FIG. 7. Comparison among Different Tip Boundaries with Free Top for: (a) Fully Embedded Piles, ω = 0; (b) Partially Embedded Piles, ω = 0

EFFECT OF BOUNDARY CONDITIONS

Figs. 7–9 show the variation of L_e' as a function of h' for different tip boundaries with a free-top boundary, fixed-with-sway top boundary, and pinned-top boundary, respectively. For

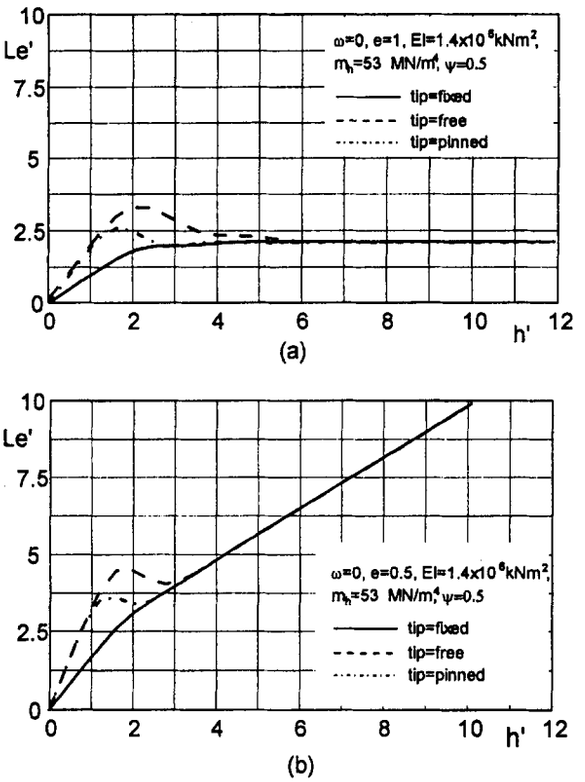

FIG. 8. Comparison among Different Tip Boundaries with Fixed-Sway Top for: (a) Fully Embedded Piles, ω = 0; (b) Partially Embedded Piles, ω = 0

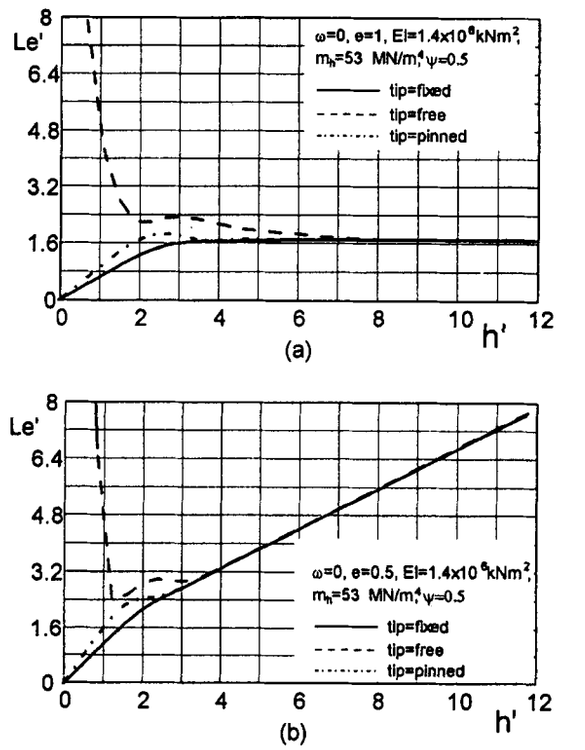

FIG. 9. Comparison among Different Tip Boundaries with Pinned Top for: (a) Fully Embedded Piles, ω = 0; (b) Partially Embedded Piles, ω = 0

the sake of comparison, the values of $\omega = 0$ and $m_h = 53$ MN/m^3 were used in the analysis. As shown in Fig. 7, as h' reached a critical value of 3.3 for fully embedded piles and 2.8 for half-embedded piles, curves representing different tip conditions but the same free-top boundary tend to coincide. Similar behavior was estimated for the cases of fixed-sway top boundary (Fig. 8) and pinned-top boundary (Fig. 9). The critical h' value for a pile with a fixed-sway top was evaluated to be 5.6 for full embedment and 3.3 for half embedment. In the pinned-top case, h' was estimated to be 7.6 for the fully embedded piles and 3.4 for the half-embedded piles. A comparison of these data, with the results presented by Gabr and Wang (1994) in which an $\omega = 1$ was used, indicated that regardless of the distribution of the horizontal subgrade reaction, the pile-top conditions mostly controlled the buckling behavior once h' reached a critical value.

In the case of the fixed-sway and pinned-top boundaries, and free-top, and pinned-tip boundaries, and for h' values between 1 and 3, the "hump" shape of the curves depicting h' as a function of L'_e was observed. As explained earlier, this shape was due to the difference in the buckling mode as compared to the fundamental case of buckling in which L'_e increased as a function of h'. In this case, the critical buckling length was less than that evaluated for the fundamental case. This rendered a lower L'_e and the consequent increase in P_{cr}.

EFFECT OF SUBGRADE REACTION

Fig. 10 shows a comparison of evaluated L_e using the different ω and m_h values utilized in the parametric study. The effect of the selected ω value on P_{cr} is pronounced. As shown in Fig. 10(a), for the free-top, fixed-tip, fully embedded condition with pile width equal to 0.75 m and embedment length (h) greater than 10, a 14% decrease in L_e was predicted as ω was increased from 0 to 0.5. Since P_{cr} varies linearly with $1/L_e^2$, the 14% decrease in L_e indicated a 28.4% increase in P_{cr}. As ω was increased from 0 to 1, a 37% decrease in L_e and, therefore, a 59% increase in P_{cr}, were predicted. For half-embedded piles with the free-top/fixed-tip condition (pile width = 0.7 m) and h greater than 10 m, a 7.4% decrease in L_e, thus a 15.5% increase in P_{cr}, was computed as ω was increased from 0 to 0.5, as shown in Fig. 10(b). As ω was increased from 0 to 1, a 14.4% decrease in L_e, thus a 28.3% increase in P_{cr}, was estimated. Comparing Fig. 10(b) with Fig. 10(a), it is evident that the effect of the selected ω value on P_{cr} is less considerable for a partially embedded pile than for a fully embedded pile. This can be explained by the fact that the contribution of the lateral soil reaction to buckling stability is more substantive in fully embedded piles as compared to partially embedded piles having the same length.

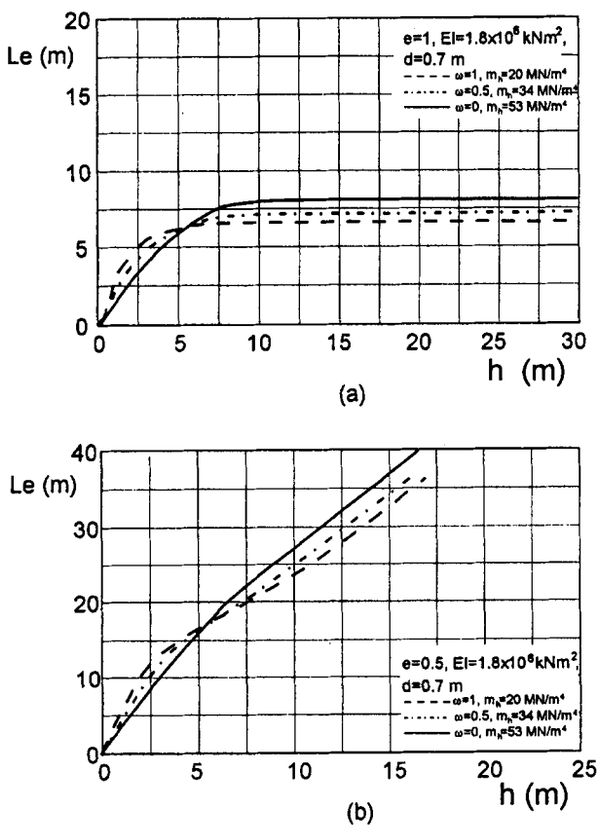

FIG. 10. Comparison among Different ω Values with Free Top and Fixed Tip for: (a) Fully Embedded Piles; (b) Half Embedded Piles

MODEL APPLICATION

The series of full-scale buckling load tests, to failure, on a 0.33 m diameter timber pile reported by Klohn and Hughes (1964) was used to verify the developed model and demonstrate its applicability. Using the structure and soil conditions given by Klohn and Hughes, the model presented in this paper was used to predict the critical buckling capacity of the test pile. The pile information and soil information utilized in the analysis are given in Table 2.

The wharf piles were driven through soft silt into an underlying dense gravel layer. The average eccentricity of the test piles was 0.127 m, with the pile top considered pinned and the pile tip fixed. Based on the soil conditions described by Klohn and Hughes, the modulus of subgrade reaction was assumed to vary as a function of depth with ω having a range of values from 0 to 1 and m_h having a range of values from 18 to 54 MN/m^4. The skin friction coefficient Ψ was assumed to vary between 0 and 1.

The predicted variation of P_{cr} as a function of Ψ for different ω and m_h values is shown in Fig. 11. The range of P_{cr} values measured by Klohn and Hughes was from 267 kN to 302.5 kN with an average of approximately 285 kN. For a given Ψ value, the estimated P_{cr} increased as ω was increased.

TABLE 2. Pile and Soil Parameters Based on Data from Klohn and Hughes (1964)

Pile Properties				Soil Properties		
L (m) (1)	h (m) (2)	d (m) (3)	E (kN/m^2) (4)	Ψ (5)	ω range (6)	m_h (MN/m^4) (7)
16.76	15.24	0.33	11.7×10^6	0–1	0–1	18–54

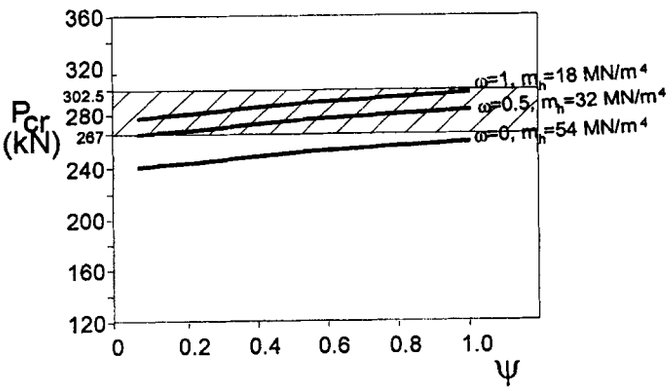

FIG. 11. Prediction of P_{cr} As Function of Skin Friction Influence Parameter for Different ω Values

In general, using $m_h = 54$ MN/m^4 and $\omega = 0$ for the distribution of the horizontal subgrade reaction underestimated the measured response. This implies that the practice of assuming an average, constant distribution of horizontal subgrade reaction should be revisited.

The comparison between the predicted and measured capacity favorably verified the applicability of the developed model. The average measured capacity of 285 kN was predicted using two combinations of ω and Ψ: $\omega = 0.5$ ($m_h = 32$ MN/m^4) and $\Psi = 0.95$; and $\omega = 1$ ($m_h = 18$ MN/m^4) and $\Psi = 0.3$.

SUMMARY AND CONCLUSIONS

A pile buckling model was developed assuming a general power distribution of the soil horizontal subgrade reaction to represent various soil conditions. The minimum potential energy method was used to develop the model with the Rayleigh-Ritz method adopted to select suitable deflection functions. Nine boundary conditions were utilized in the model. A parameter study was conducted to analyze the effect of the pile top and tip conditions and the horizontal subgrade reaction distribution on the equivalent buckling length and the buckling capacity. Applicability of the developed model was investigated through the use of Klohn and Hughes' (1964) results from full-scale buckling load tests to failure. Based on the analysis and results presented in this study, the following conclusions are advanced:

1. Regardless of the distribution of the horizontal subgrade reaction, the boundary conditions of the pile tip had a minimal effect on the critical buckling loads in cases where h' exceeded a critical value. In the case of fully embedded piles, this value was approximately 3.3 for the free-top condition, 5.6 for the fixed-with-sway top condition, and 7.6 for the pinned-top condition. Similar behavior was estimated for partially embedded piles.
2. In the case of fixed-sway top, free-tip, and pinned-tip conditions, an increase in P_{cr} was estimated as h' was varied between 1 and 3. The "hump" shape obtained for several of the h'-L_e' curves was explained based on the first buckling modes and the presence of inflection points along the pile.
3. The effect of the selected ω value on P_{cr} is pronounced. For the free-top, fixed-tip, and fully embedded conditions with the embedment length (h) greater than 10 m (pile width = 0.7 m), a 59% increase in P_{cr} was predicted as ω was increased from 0 to 1.
4. For the half-embedded piles with the free-top/fixed-tip condition and h greater than 10 m (pile width = 0.7 m), a 28.3% increase in P_{cr} was observed as ω was increased from 0 to 1. The effect of ω value on P_{cr} is less considerable for partially embedded piles than for fully embedded piles.
5. A comparison between the results of pile load tests reported in the literature and the model presented in this paper favorably verified the applicability of the model.

APPENDIX I. COEFFICIENT DETERMINANTS AND THEIR COMPONENTS

For the boundary condition a (free top-fixed tip), as shown in Fig. 2(a), the coefficient determinant is expressed as follows:

$$\Delta = \begin{vmatrix} b_{1,1} - P' & b_{1,2} & b_{1,3} & \cdots & b_{1,n} \\ b_{2,1} & b_{2,2} - P' & b_{2,3} & \cdots & b_{2,n} \\ \cdots & \cdots & \cdots & \cdots & \cdots \\ b_{n,1} & b_{n,2} & b_{n,3} & \cdots & b_{n,n} - P' \end{vmatrix} = 0 \quad (14)$$

where

$$P' = \frac{PL^2}{\Pi^2 EI} \quad (15)$$

and $b_{i,j}$ = intermediate parameters for calculation. The ranges of i, j and values of $b_{i,j}$ are different depending on the boundary conditions. Here, for boundary condition a

$$b_{i,i} = \omega i^2 + a_{i,i}A + t_{i,i}B \quad (16a)$$

$$b_{i,j} = b_{i,j} = a_{i,j}A + t_{i,j}B \quad (16b)$$

where $i = 1, 2, \ldots, n$; $j = i + 1, i + 2, \ldots, n$; both A and B are nondimensional; and embedment ratio $e = h/L$.

$$A = 2\left(\frac{\alpha L}{\Pi\zeta}\right)^4; \quad B = \frac{2\psi e^3}{3\Pi^3} \quad (17)$$

and

$$a_{i,j} = \frac{1}{(i - 0.5)(j - 0.5)}\left\{\frac{\Pi}{2}e^2 - \frac{1 - \cos[(i - 0.5)e\Pi]}{(i - 0.5)^2\Pi} - \frac{1 - \cos[(j - 0.5)e\Pi]}{(j - 0.5)^2\Pi} + \frac{1 - \cos[(i + j - 1)e\Pi]}{2(i + j - 1)^2\Pi} + \frac{1 - \cos[(i - j)e\Pi]}{2(i - j)^2\Pi}\right\} \quad (18)$$

$$t_{i,j} = \frac{1 - \cos[(i - j)e\Pi]}{2(i - j)^2} - \frac{1 - \cos[(i + j - 1)e\Pi]}{2(i + j - 1)^2} \quad (19)$$

In both (18) and (19) $i = 1, 2, 3, \ldots, n$; and $j = i, i + 1, i + 2, \ldots, n$.

For boundary condition e (fixed-sway top-free tip), as shown in Fig. 2(e), the coefficient determinant is expressed as follows:

$$\Delta = \begin{vmatrix} \frac{\Pi e^2}{2A} & d_1 & d_2 & d_3 & \cdots & d_n \\ d_1 & b_{1,1} - P' & b_{1,2} & b_{1,3} & \cdots & b_{1,n} \\ d_2 & b_{2,1} & b_{2,2} - P' & b_{2,3} & \cdots & b_{2,n} \\ \cdots & \cdots & \cdots & \cdots & \cdots & \cdots \\ d_n & b_{n,1} & b_{n,2} & b_{n,3} & \cdots & b_{n,n} - P' \end{vmatrix} = 0 \quad (20)$$

where d_j, $b_{i,j}$ = intermediate parameters for calculation.

$$d_j = \frac{1}{(j - 0.5)^2}\left\{e - \frac{\sin[(j - 1)e\Pi]}{(j - 1)\Pi}\right\} \quad (21)$$

where $j = 1, 2, \ldots, n$; and

$$b_{i,i} = \omega(i - 0.5)^2 + a_{i,i}A + t_{i,i}B \quad (22a)$$

$$b_{i,j} = b_{i,j} = a_{i,j}A + t_{i,j}B \quad (22b)$$

where $i = 1, 2, \ldots, n$; $j = i + 1, i + 2, \ldots, n$; and

$$a_{i,j} = \frac{1}{2(i - 0.5)(j - 0.5)\Pi}\left\{\frac{1 - \cos[(i - j)e\Pi]}{(i - j)^2} - \frac{1 - \cos[(i + j - 1)e\Pi]}{(i + j - 1)^2}\right\} \quad (23)$$

$$t_{i,j} = \frac{1 - \cos[(i + j - 1)e\Pi]}{2(i + j - 1)^2} + \frac{1 - \cos[(i - j)e\Pi]}{2(i - j)^2} \quad (24)$$

In both (23) and (24) $i = 1, 2, 3, \ldots, n$; and $j = i, i + 1, i + 2, \ldots, n$.

For boundary condition g (pinned top-fixed tip), as shown in Fig. 2(g), the coefficient determinant is expressed as follows:

$$\Delta = \begin{vmatrix} b_{1,1} - (2 \times 1^2 + 0.5)P' & b_{1,2} + (1 + 0.5)^2P' & b_{1,3} & b_{1,4} & \cdots & b_{1,n} \\ b_{1,2} + (1 + 0.5)^2P' & b_{2,2} - (2 \times 2^2 + 0.5)P' & b_{2,3} + (2 + 0.5)^2P' & b_{2,4} & \cdots & b_{2,n} \\ b_{1,3} & b_{2,3} + (2 + 0.5)^2P' & b_{3,3} - (2 \times 3^2 + 0.5)P' & b_{3,4} + (3 + 0.5)^2P' & \cdots & b_{3,n} \\ b_{1,4} & b_{2,4} & b_{3,4} + (3 + 0.5)^2P' & b_{4,4} - (2 \times 4^2 + 0.5)P' & \cdots & b_{4,n} \\ \cdots & \cdots & \cdots & \cdots & \cdots & \cdots \\ b_{1,n} & b_{2,n} & b_{3,n} & b_{4,n} & \cdots & b_{n,n} - (2n^2 + 0.5)P' \end{vmatrix} = 0 \quad (25)$$

where $b_{i,j}$ = intermediate parameters for calculation; and

$$b_{i,i} = \omega(i + 0.5)^4 + \omega(j - 0.5)^4 + a_{i,i}A + t_{i,i}B \quad (26a)$$

$$b_{i,j} = a_{i,j}A - t_{i,j}B \quad (26b)$$

where $i = 1, 2, \ldots, n$; $j = i + 2, i + 3, \ldots, n$; and

$$b_{i,i+1} = a_{i,i+1}A - \omega(i + 0.5)^4 + t_{i,i+1}B \quad (27)$$

$$a_{i,j} = \frac{1}{2}\Pi\left\{\frac{1 - \cos[(i + j + 1)e\Pi]}{(i + j + 1)^2} + \frac{1 - \cos[(i + j - 1)e\Pi]}{(i + j - 1)^2} - \frac{1 - \cos[(i - j + 1)e\Pi]}{(i - j + 1)^2} - \frac{1 - \cos[(i - j - 1)e\Pi]}{(i - j - 1)^2} + \frac{2 - 2\cos[(i - j)e\Pi]}{(i - j)^2} - \frac{2 - 2\cos[(i + j)e\Pi]}{(i + j)^2}\right\} \quad (28)$$

$$t_{i,j} = \frac{(ij - 0.25)\{1 - \cos[(i + j)e\Pi]\}}{(i + j)^2} + \frac{(ij + 0.25)\{1 - \cos[(i - j)e\Pi]\}}{(i - j)^2} - \frac{(i - 0.5)(j - 0.5)\{1 - \cos[(i + j - 1)e\Pi]\}}{2(i + j - 1)^2} - \frac{(i + 0.5)(j + 0.5)\{1 - \cos[(i + j + 0.5)e\Pi]\}}{2(i + j + 1)^2} + \frac{(i - 0.5)(j + 0.5)\{1 - \cos[(i - j - 1)e\Pi]\}}{2(i - j - 1)^2} - \frac{(i + 0.5)(j - 0.5)\{1 - \cos[(i - j + 1)e\Pi]\}}{2(i - j + 1)^2} \quad (29)$$

where $i = 1, 2, 3, \ldots, n$; and $j = i, i + 1, i + 2, \ldots, n$.

APPENDIX II. REFERENCES

Bergfelt, A. (1957). "The axial and lateral load bearing capacity, and failure by buckling of piles in soft clay." *Proc., 4th Int. Conf. on Soil Mech. and Found. Engrg.*, 8–13.

Brandtzaeg, A., and Harboe, E. (1957). "Buckling tests of slender steel piles in soft, quick clay." *Proc., 4th Int. Conf. on Soil Mech. and Found. Engrg.*, 19–23.

Chajes, A. (1974). *Principles of structural stability theory*. Prentice-Hall, Inc., Englewood Cliffs, N.J.

Davisson, M. T., and Prakash, S. (1963). "A review of soil-pile behavior." *Hwy. Res. Rec.*, 39, 25–48.

Davisson, M. T., and Robinson, K. E. (1965). "Bending and buckling of partially embedded piles." *Proc., 6th Int. Conf. on Soil Mech. and Found. Engrg.*, 2, 243–246.

Gabr, M. A., and Wang, J. (1994). "Buckling of friction piles supporting bridge foundations." *Transp. Res. Rec. 1447*, Transportation Research Board, Washington, D.C., 93–101.

Golder, H. G., and Skipp, B. O. (1957). "The buckling of piles in soft clay." *Proc., 4th Int. Conf. on Soil Mech. and Found. Engrg.*, 35–39.

Japanese Road Association. (1976). "Road bridge substructural design, designing of pile foundation." *Annu. Rep. on Deep Found.*, Tokyo.

Kubo, J. (1965). "Experimental study of the behavior of laterally loaded piles." *Proc., 6th Int. Conf. on Soil Mech. and Found. Engrg.*, Montreal, 2, 275–279.

Prakash, S., and Sharma, H. D. (1990). *Pile foundations in engineering practice*. John Wiley & Sons, Inc., New York, N.Y.

Reddy, A. S., and Valsangkar, A. J. (1970). "Buckling of fully and partially embedded piles." *J. Soil Mech. and Found. Div.*, ASCE, 96(6), 1951–1965.

Reese, L. C., and Matlock, H. (1956). "Non-dimensional solutions for laterally loaded piles with soil modulus assumed proportional to depth." ASTM, Philadelphia, Pa., STP 444, 160–176.

Rowe, P. W. (1956). "The single pile subject to horizontal force." *Geotechnique*, 6, 70–85.

Terzaghi, K. (1955). "Evaluation of coefficients of subgrade reaction." *Geotechnique*, 5, 297–326.

APPENDIX III. NOTATION

The following symbols are used in this paper:

- d = pile width or diameter;
- EI = flexural stiffness of pile;
- e = embedment ratio, h/L;
- h = embedded pile length;
- h' = nondimensional embedded length of pile, αh;
- k_h = coefficient of horizontal subgrade reaction;
- L = total pile length;
- L' = nondimensional length of pile, αL;
- L'_e = nondimensional equivalent buckling length, αL_e;
- m_h = ratio between coefficient of horizontal subgrade reaction and depth below surface, value of which depends on relative density of soil, kN/m^4;
- n = number of half-wave of deflection function, integer;
- P = axial load;
- $P(x)$ = axial force;
- $q(x)$ = horizontal soil reaction per unit length of pile, kN/m;
- x = distance from pile tip;
- y = lateral pile deflection;
- α = coefficient of pile-soil compliancy or relative stiffness;
- ψ = parameter defining influence of skin friction on pile axial force distribution with 0 value representing no skin friction considered; and
- ω = empirical index equal to or greater than zero.